



## ORIGINAL ARTICLE

# Tetraethylenepentamine-containing adsorbent with optimized amination efficiency based on grafted polyolefin microfibrinous substrate for CO<sub>2</sub> adsorption



Noor Ashikin Mohamad<sup>a,b</sup>, Mohamed Mahmoud Nasef<sup>a,b,\*</sup>, Pooria Moozarm Nia<sup>b</sup>, Nur Afifah Zubair<sup>a,b</sup>, Arshad Ahmad<sup>b,c</sup>, Tuan Amran Tuan Abdullah<sup>b,c</sup>, Roshafima Rasit Ali<sup>a,b</sup>

<sup>a</sup> Malaysia-Japan International Institute of Technology, Universiti Teknologi Malaysia, Jalan Sultan Yahya Petra, 54100 Kuala Lumpur, Malaysia

<sup>b</sup> Advanced Materials Research Group, Center of Hydrogen Energy, Universiti Teknologi Malaysia, Jalan Sultan Yahya Petra, 54100 Kuala Lumpur, Malaysia

<sup>c</sup> Department of Chemical Engineering, Universiti Teknologi Malaysia, 81310 Johor Bahru, Malaysia

Received 13 December 2020; accepted 7 February 2021

Available online 17 February 2021

## KEYWORDS

Solid aminated adsorbent;  
Polyolefin substrate;  
Tuning amination level;  
Taguchi method;  
CO<sub>2</sub> capture

**Abstract** Preparation and optimization of tetraethylenepentamine (TEPA) content in polyethylene/polypropylene (PE/PP) grafted with poly(glycidyl methacrylate) (PGMA) adsorbent for CO<sub>2</sub> capture were investigated. The amination reaction parameters such as solvent type, amine to solvent ratio and reaction time were optimized using the Taguchi method to maximize the level of amination in the adsorbent. The obtained data were statistically analysed using the analysis of variance (ANOVA) and signal to noise (S/N) ratio. The chemical, morphological, structural, and thermal properties of the aminated fibrous adsorbent were investigated using Fourier transform infrared (FTIR), scanning electron microscope (SEM), X-ray diffraction (XRD) and thermal gravimetric analysis (TGA). The performance of the obtained TEPA-containing fibrous adsorbent was evaluated for adsorption of pure and mixed CO<sub>2</sub>/N<sub>2</sub> gases under varying pressure up to 30 bar. The optimization of the amination parameters led to an adsorbent with improved properties in forms of not only 23% higher amination level and 27% greater TEPA utilisation efficiency but also 31.6% bigger

\* Corresponding author at: Malaysia-Japan International Institute of Technology, Universiti Teknologi Malaysia, Jalan Sultan Yahya Petra, 54100 Kuala Lumpur, Malaysia.

E-mail address: [mahmoudeithar@cheme.utm.my](mailto:mahmoudeithar@cheme.utm.my) (M.M. Nasef).

Peer review under responsibility of King Saud University.



CO<sub>2</sub> adsorption capacity than its corresponding adsorbent obtained without optimization. The adsorbent also demonstrated high CO<sub>2</sub>/N<sub>2</sub> selectivity and regeneration stability. The results suggest that the obtained TEPA-containing fibrous adsorbent is a promising candidate for CO<sub>2</sub> capture from CO<sub>2</sub>/N<sub>2</sub> gaseous mixture under various pressures.

© 2021 The Author(s). Published by Elsevier B.V. on behalf of King Saud University. This is an open access article under the CC BY-NC-ND license (<http://creativecommons.org/licenses/by-nc-nd/4.0/>).

## 1. Introduction

Development of highly efficient materials and processes for CO<sub>2</sub> capture has been widely investigated for mitigation of CO<sub>2</sub> emission, which is continuously rising by the soaring demand on fossil (Andreoli, 2017). Majority of CO<sub>2</sub> emissions come from energy production (55%) which is driven by fossil fuel (natural gas, petroleum, and coal) combustion and its capturing in industrial power plants follows 3 main approaches pre-combustion, post-combustion and oxyfuel combustion (Leung et al., 2014). Various technologies using chemical and physical solvents, solid adsorbents and membrane separators have been employed to capture CO<sub>2</sub> from various effluents (Luis Míguez et al., 2018). Chemical absorption with aqueous alkanolamine solutions is the most matured technology due to high CO<sub>2</sub> capturing efficiency and selectivity at low partial pressure (Abu-Zahra et al., 2013). However, this process is challenged by high-energy demand, equipment corrosion and high operation cost (Petrovic et al., 2020). Thus, adsorption by solid support materials such as activated carbon, zeolites, metal organic frameworks (MOFs), porous and mesoporous silica and functionalized polymer supports, has been proposed as reliable alternative adsorbents materials for CO<sub>2</sub> capture (Jafari et al., 2018; Zhang et al., 2019). Adsorbents are commonly hosted in columns which operated based on pressure swing adsorption, temperature swing adsorption, vacuum swing adsorption or electric swing adsorption, which varies depending on the adsorbent regeneration strategy (Songolzadeh et al., 2014).

Porous supports fall into micro- and nano-scaled categories and possess advantages in terms of large surface area, high chemical stability and high CO<sub>2</sub> selectivity when functionalized with chemical groups such as amines (Luo et al., 2016). Particularly, solid fibrous supports are suitable for hosting amines using techniques like physical (impregnation) and chemical (grafting) interactions. The former method has the disadvantage of not only slow adsorption rate caused by diffusion limitation accompanied pore-filling with amines but also amine leaching and evaporation as a result of weak physical interactions with porous support (Jahandar Lashaki et al., 2019; Liu et al., 2018). On the other hand, chemical grafting leads to stable adsorbents with better kinetics compared to physically impregnated ones but with lower CO<sub>2</sub> adsorption capacity (Varghese and Karanikolos, 2020). Thus, chemical impregnation of amine is highly advantageous for adsorbent development and the level of amination must be carefully optimized. Free radical grafting is an appealing method for covalent incorporation of amine-containing grafts to various polymeric substrates and can be carried out using chemical, photochemical, plasma or radiochemical initiators. This method allows desired control to the type of the grafting monomer and amine groups providing tailored adsorbents with desired properties. Radiation induced graft copolymerization (RIGC) is a versa-

tile method to impart desired chemical moiety to inert fibrous polymer substrates by grafting with vinylic (e.g. vinyl benzyl chloride) or acrylate monomers such as glycidyl methacrylate (GMA) (Nasef and Güven, 2012).

Grafting of GMA introduces epoxy groups to various fibrous polymer substrates such as polyethylene/polypropylene (PE/PP) nonwoven sheets and PP nanofibrous sheets, which undergo a mild ring-opening reaction such as amination converting the grafted PGMA precursor into CO<sub>2</sub> adsorbent (Abbasi et al., 2019b, 2018; Nasef et al., 2014b, 2014a). The selection of polyolefins such as PE/PP substrate is motivated by its low cost, abundance, stability, great process ability and high radiation resistance (Graziano et al., 2018). The performance of the obtained adsorbents is mainly controlled by the type of amine and its loading level. Particularly, the amine loading level is a function of amination reaction parameters such as concentration of amine agent, type of diluting solvent, temperature and reaction time. Hence, it is essential to optimize the amination reaction parameters to incorporate the desired level of amine (amine density). Tetraethylene pentamine (TEPA) is a branched polyamine that has abundant amino functional groups and potential to enhance CO<sub>2</sub> adsorption of TEPA impregnated solid porous inorganic substrates such as nanosepiolite (Irani et al., 2015) and mesocellular silica sponge (Dao et al., 2020). However, amination of the PGMA grafted fibrous substrates with TEPA and optimization of its density have not been reported.

Design of experiment (DOE) is a statistical tool than was used in a number of studies as a tool for optimization of the treatment parameters to maximize CO<sub>2</sub> adsorption capacity in amine containing adsorbents through applying response surface methodology (RSM) (Selin and Emik, 2018; Thouchprasitchai et al., 2017). However, studies employing DOE through Taguchi method for maximizing the amine level to enhance CO<sub>2</sub> adsorption performance have not been reported. Taguchi method, is a unique and powerful technique that allows economical optimization of process parameters with minimum number of experiments to determine the best factor combination by studying the effects of individual factors on the response (Davis and John, 2018).

The objective of this study is to systematically investigate the effect of reaction parameters on amination efficiency of PGMA grafted PE/PP fibrous substrate obtained by RIGC of GMA using Taguchi method. Particularly, the parameters of amination with TEPA such as solvent types, amine to solvent ratio and reaction time are optimized to achieve a maximum level of amination. The various physico-chemical properties of the obtained adsorbent are investigated. The theoretical CO<sub>2</sub> adsorption, TEPA utilisation efficiency and adsorbent selectivity are studied. The performance of the obtained adsorbent with optimum amine content was evaluated for CO<sub>2</sub> adsorption.

## 2. Experimental section

### 2.1. Chemicals and reagents

The PE/PP nonwoven sheet grafted with PGMA with a degree of grafting of 166%, was prepared by RIGC as described in a previous communication (Nasef et al., 2014a). The PE/PP sheets were irradiated by an electron beam (EB) accelerator (NHV-Nissin High Voltage, EPS3000) operated at an acceleration energy of 2 MeV and a beam current of 10 mA with a total dose of 50 kGy at 25 kGy/pass to create the free radicals. The irradiated PE/PP sheets were placed in a grafting system having an evacuated glass ampoule containing N<sub>2</sub> bubbled emulsion grafting mixture containing 10% vol% of GMA in deionized water (DI) and 0.5% Tween 20 (surfactant). The reaction was carried out at a temperature of 50 °C for 35 min and the obtained grafted samples are denoted as PE/PP-g-PGMA. The degree of grafting in the samples was determined as the weight increase after grafting compared to initial sample weight. TEPA (purity ≥ 95%) was purchased from Acros Organics (California, United States). Solvents such as methanol, ethanol and isopropanol were analytical grade and purchased from Merck (Darmstadt, Germany). DI was obtained from Barnstead Nanopure Diamond Lab Water Purification System (ThermoFisher, Waltham, USA) and used for washing of samples and dilution of TEPA. Pure CO<sub>2</sub> gas (99.8%) and pure N<sub>2</sub> gas (99.999%) were supplied by Linde Malaysia (Sdn Bhd).

### 2.2. Functionalization of adsorbent precursors

A sample of known weight of PE/PP-g-PGMA sheet (adsorbent precursors) in a form small pieces of known weight was added to a 100 ml round bottom flask containing 30 ml of TEPA solutions having different solvents (water, methanol, ethanol, and isopropanol) and TEPA/solvent ratios as shown in Table 1. The reaction was carried out under reflux taking the boiling point of each solvent (100 °C, 65 °C, 78 °C and 82 °C) into account and at continuous stirring for a time range of 1–4 h. After reaction completion, the aminated sample was removed and repeatedly washed with DI and ethanol followed by drying in a vacuum oven at 60 °C for 5 h. All experiments were repeated 3 times and the reported data for the percent of amination is an average of three readings. The weight change in the sample after amination reaction, which is denoted as PE/PP-g-PGMA/TEPA was determined and used to calculate the amination efficiency (percent of amination) as per the following equation:

$$\text{Amination efficiency} = \frac{(W_a - W_g)/MW_{TEPA}}{(W_g - W_p)/MW_{GMA}} \times 100\% \quad (1)$$

where MW<sub>GMA</sub> is molecular weight of GMA and MW<sub>TEPA</sub> is the molecular weight of TEPA. W<sub>p</sub>, W<sub>g</sub> and W<sub>a</sub> are the weights of pristine, grafted and aminated PE/PP substrates, respectively.

### 2.3. Characterization of adsorbent

The chemical, morphological, textural, structural, and thermal properties of the aminated fibrous adsorbent were evaluated in comparison of the pristine PE/PP and the grafted fibrous substrates before functionalization. The changes in the chemical composition were analysed using a Nicolet iS50 FT-IR spectrometer. The spectra were obtained in a frequency range of 500–4000 cm<sup>-1</sup> with 32 scans and 4 cm<sup>-1</sup> resolution. The morphological properties of the samples were investigated using a GEMINISEM 500 microscope. The textural properties were obtained from nitrogen adsorption/desorption isotherms recorded at -196 °C on Quantachrome NOVAtouch™ instrument. The surface area, total pore volume and pore size were measured by using the multipoint Brunauer–Emmett–Teller (BET) method. The crystalline structure of the samples was investigated by X-ray diffraction (XRD) using a PANalytical Empyrean analyser at Bragg's angle in the range of 5–80°. The thermal stability of the samples was carried out using a Q50 thermogravimetric analyser (TA Instruments) in a temperature range of 30–700 °C at a heating rate of 10 °C /min.

### 2.4. Design of experiment (DOE)

Before designing the experiment, a few initial experiments were performed to screen the significant independent parameters and find their suitable levels. Based on the literature analysis and preliminary experimental results, the significant parameters were identified, and their levels were determined as presented in Table 1 (Abbasi et al., 2019b; Othman et al., 2019). The experimental design was set to maximize the amination percentage and thus a quality characteristic was employed for the analysis. Three experimental parameters such as solvent type, TEPA/solvent ratio and reaction time were investigated and optimized through Taguchi design. The analysis of variance (ANOVA) and signal-to-noise (S/N) (available in Mini-tab 17.0 software) were used to monitor the effect of the parameters on amination efficiency and optimize the process. Experimental runs were designed through Taguchi orthogonal array method of L16.

**Table 1** Amination reaction parameters and their levels.

Variables	Levels			
	1	2	3	4
Solvent type	Water	Methanol	Ethanol	Isopropanol
TEPA/solvent ratio	1:3	1:1	2:1	3:1
Reaction time (h)	1	2	3	4

### 2.5. CO<sub>2</sub> adsorption tests

The CO<sub>2</sub> adsorption capacity measurement studies was carried out using the magnetic suspension balance (MSB) from isoSORP® Gravimetric Analyzer that was manufactured by RUBOTHERM (Bochum, Germany). Details of the basic principles, components and operational procedure of MSB was described elsewhere (Fujii et al., 2010; Schell et al., 2012). Completion of one cycle of CO<sub>2</sub> adsorption capacity measurement consists of three steps comprising pre-treatment, buoyancy, and adsorption measurement. All the data were recorded by RUBOTHERM system control software (RSCS-2016) and each measurement was configured step by step. A pre-treatment was conducted for both fresh and regenerated adsorbent samples by heating 80 °C for 4.5 h under vacuum until the weight loss of adsorbent became constant indicating a complete removal of any trapped moisture in the former and adsorbed CO<sub>2</sub> in the latter. Buoyancy measurement was also carried out for fresh and regenerated samples to precisely determine the adsorbents weight and volume using purified N<sub>2</sub> gas at 30 °C in a varying pressure from vacuum condition to 30 bar. Finally, the adsorption measurements of both pure CO<sub>2</sub> and N<sub>2</sub> gases and their mixture containing 40% CO<sub>2</sub> was carried out by the sample evacuation for 30 to 60 min followed by gas introduction variation of the pressure from 5 to 30 bar with a gas flowrate of 500 ml/min at 30 °C. The equilibrium sorption was achieved in about 50 min for every pressure reading. Desorption is carried after each adsorption measurement was completed at 30 bars. The desorption process was performed by depressurizing sample holding vessel until reaching vacuum before heating to 80 °C for 4.5 h until no weight loss was detected in the adsorbents. This was followed by buoyancy and adsorption measurements to achieve another adsorption cycle. All adsorption/desorption

cycles experiments were repeated 3 time and the average values were reported.

### 2.6. Calculation of theoretical CO<sub>2</sub> adsorption, TEPA utilisation efficiency and selectivity

The theoretical CO<sub>2</sub> adsorption capacity ( $v_T$ ) in mg/g of the adsorbent (PP/PP-g-PGA/TEPA) was calculated taking the reaction of  $2RNH_2 + CO_2 \rightarrow R_2NH_2^+ + R_2NCOO^-$  (in the absence of water) into account using equation (2) (Guo et al., 2020):

$$v_T = \frac{W_a - W_g/W_a}{MW_{TEPA}} \times 2.5 \times M_{CO_2} \quad (2)$$

where  $M_{CO_2}$  is the molecular weight of CO<sub>2</sub> (44 g/mol).

The TEPA utilization efficiency or adsorption capacity per unit TEPA ( $Q$ ) in mg/g, which refers to the amount of adsorbed CO<sub>2</sub> per unit of loaded TEPA, can be calculated as follows (Guo et al., 2020):

$$Q = \frac{v}{w} \quad (3)$$

where  $v$  is the measured CO<sub>2</sub> adsorption capacity (mg/g) and  $w$  is the TEPA loading ratio (%).

The adsorption selectivity was calculated using the following equation:

$$Selectivity = \frac{v_{CO_2}/v_{N_2}}{P_{CO_2}/P_{N_2}} \quad (4)$$

$v_{CO_2}$  and  $v_{N_2}$  are the experimental adsorption capacities (mg/g) of pure CO<sub>2</sub> and N<sub>2</sub>, respectively.  $P_{CO_2}$  is partial pressure of CO<sub>2</sub> and  $P_{N_2}$  is partial pressure of N<sub>2</sub>.

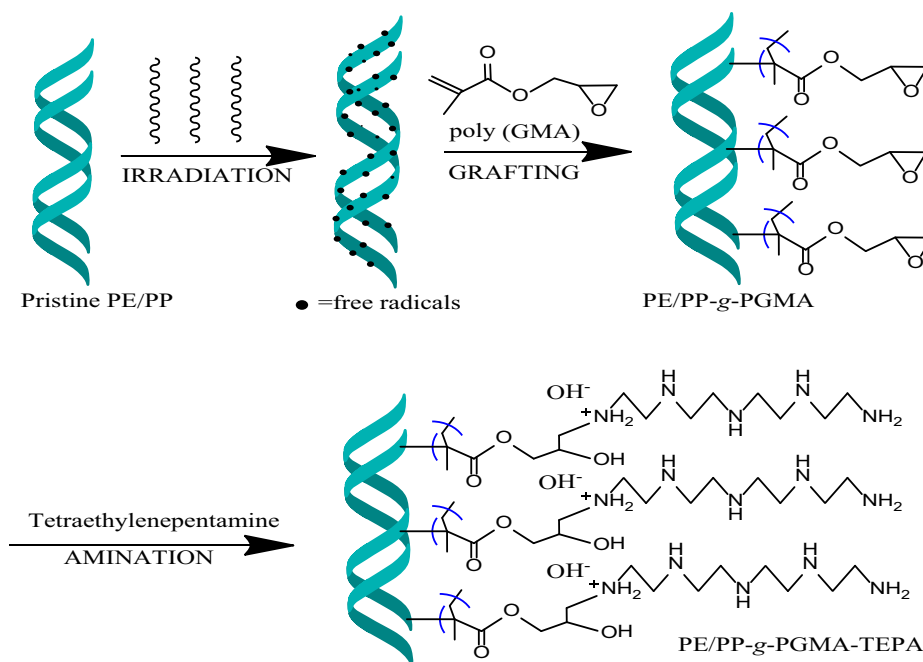


**Fig. 1** Reaction scheme for preparation of fibrous adsorbent by RIGC of GMA onto PE/PP nonwoven sheet and subsequent amination with TEPA.

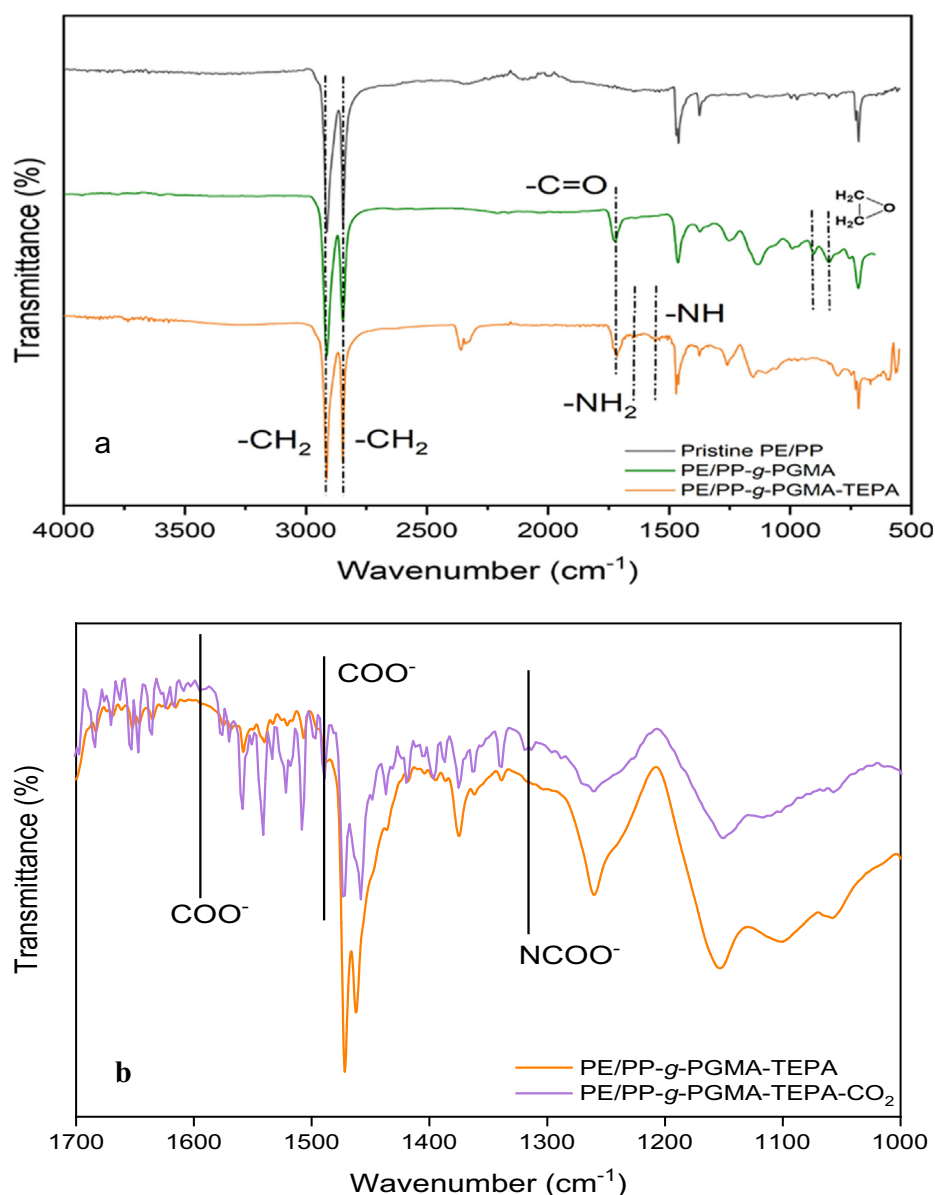
### 3. Results and discussion

Fig. 1 shows reaction scheme for preparation of CO<sub>2</sub> fibrous adsorbents by RIGC of GMA onto PE/PP fibrous sheet and subsequent functionalization of the obtained PE/PP-g-PGMA with TEPA. The incorporation of TEPA conferred the basicity in forms of polyamines which are essential for CO<sub>2</sub> capture (chemisorption) which is categorized as Lewis acid (Varghese and Karanikolos, 2020).

#### 3.1. Changes in chemical structure

Fig. 2a shows the spectra of pristine PE/PP and PGMA grafted PE/PP nonwoven sheets together with the corresponding aminated adsorbent. The pristine PE/PP polymer was marked by the presence of 2 peaks representing the

antisymmetric and asymmetric stretching vibrations of C-H at 2917 and 2847 cm<sup>-1</sup>, respectively. This was coupled with bending vibration peaks at 1457 cm<sup>-1</sup> for CH<sub>2</sub> and 1376 cm<sup>-1</sup> for CH<sub>3</sub> of PP (Kavakli et al., 2014). The incorporation of PGMA led to the emergence of 2 new bands at 840 and 905 cm<sup>-1</sup>, which are assigned for epoxy group confirming the presence of successful grafting (Nasef et al., 2014a). Besides, the peak at 1740 cm<sup>-1</sup> was assigned for the carbonyl groups from the ester in PGMA present in both PE/PP-g-PGMA and PE/PP-g-PGMA/TEPA samples (Kavakli et al., 2016). The disappearance of epoxy group representative bands at 840 and 905 cm<sup>-1</sup> after amination provides a strong evidence for the successful epoxy ring-opening by TEPA. The peaks at 1527 cm<sup>-1</sup> and 1658 cm<sup>-1</sup> were assigned for the secondary and primary amine from TEPA. From these results, it can be concluded that a fibrous adsorbent was successfully



**Fig. 2** FTIR spectra of: (a) pristine PE/PP, PE/PP-g-PGMA and PE/PP-g-PGMA/TEPA samples and (b) adsorbent of before and after CO<sub>2</sub> adsorption.

prepared by PGMA grafting and subsequent amination. Furthermore, an investigation of the changes took place in the adsorbent chemical structure after CO<sub>2</sub> adsorption compared to pristine adsorbent was made and the obtained spectra are shown in Fig. 2b. The adsorbent spectrum showed 2 new peaks at 1590 cm<sup>-1</sup> and 1490 cm<sup>-1</sup>, which are assigned for COO<sup>-</sup> stretching vibrations after capturing of CO<sub>2</sub> molecules by the adsorbent. The appearance of a small peak at 1320 cm<sup>-1</sup> originated from the formation of carbamate (NCOO<sup>-</sup>) skeletal vibration confirms the interaction of CO<sub>2</sub> with the TEPA amine group (Dao et al., 2020; Wang et al., 2020).

### 3.2. Changes in surface morphology

Fig. 3 shows the changes in the surface morphology of PE/PP-g-PGMA/TEPA compared to pristine PE/PP substrate and that of the corresponding grafted PE/PP-g-PGMA precursor. The average of fibre diameter of pristine PE/PP substrate was increased significantly after grafting of PGMA and covalent impregnation of TEPA. For instance, the average of fiber diameter increased from 12.89 μm in pristine PE/PP to 20.92 μm in PE/PP-g-PGMA and to 32.54 μm in PE/PP-g-PGMA/TEPA. This was accompanied by a reduction in the free volume (pores) between the fibers forming denser and lesser porous structure in the adsorbent sheet. These observations further confirm the success of PGMA grafting and TEPA loading.

From the previous sample analysis, the chemical and textural properties of the best PE/PP-g-PGMA/TEPA adsorbent can be summarized as presented in Table 2. As can be seen, the adsorbent has a small surface area compared to inorganic porous aminated adsorbents reported in the literature. However, the adsorption in this material is rather dependent upon the large number of amine groups present on its fibrous surfaces. This suggests that CO<sub>2</sub> adsorption is not only predominantly controlled by the number of the polyamine ligands and their distribution on the surface of the adsorbent but also by the amine sites accessibility.

### 3.3. Changes in crystalline structure

Fig. 4 shows the XRD diffractograms of the pristine PE/PP, PE/PP-g-PGMA and PE/PP-g-PGMA/TEPA samples. All the diffractograms showed almost similar crystalline peak patterns without significant changes in the intensities of major peaks indicating that the crystalline structure of pristine PE/PP was well-preserved even after the two-step procedure, i.e. grafting and amination. Moreover, there is no new peak emerged after the amination of PE/PP-g-PGMA precursor confirming that amines has no contribution to diffraction pattern (Hashim, 1998; Sharif et al., 2013). However, the diffraction angles showed minor shifts to higher Bragg's angle after incorporation of PGMA and subsequent amination with TEPA. These observations suggest that the grafting of GMA took place in areas close to the surface of the crystallites of PE/PP substrate causing a partial disorder in the crystalline structure which slightly increased with loading of TEPA. It can be concluded that the incorporation of PGMA/TEPA ligand took place mainly on the surfaces of PE/PP fibrous support in a way affecting the porous structure of the sheet without invading the core structure of the fibers.

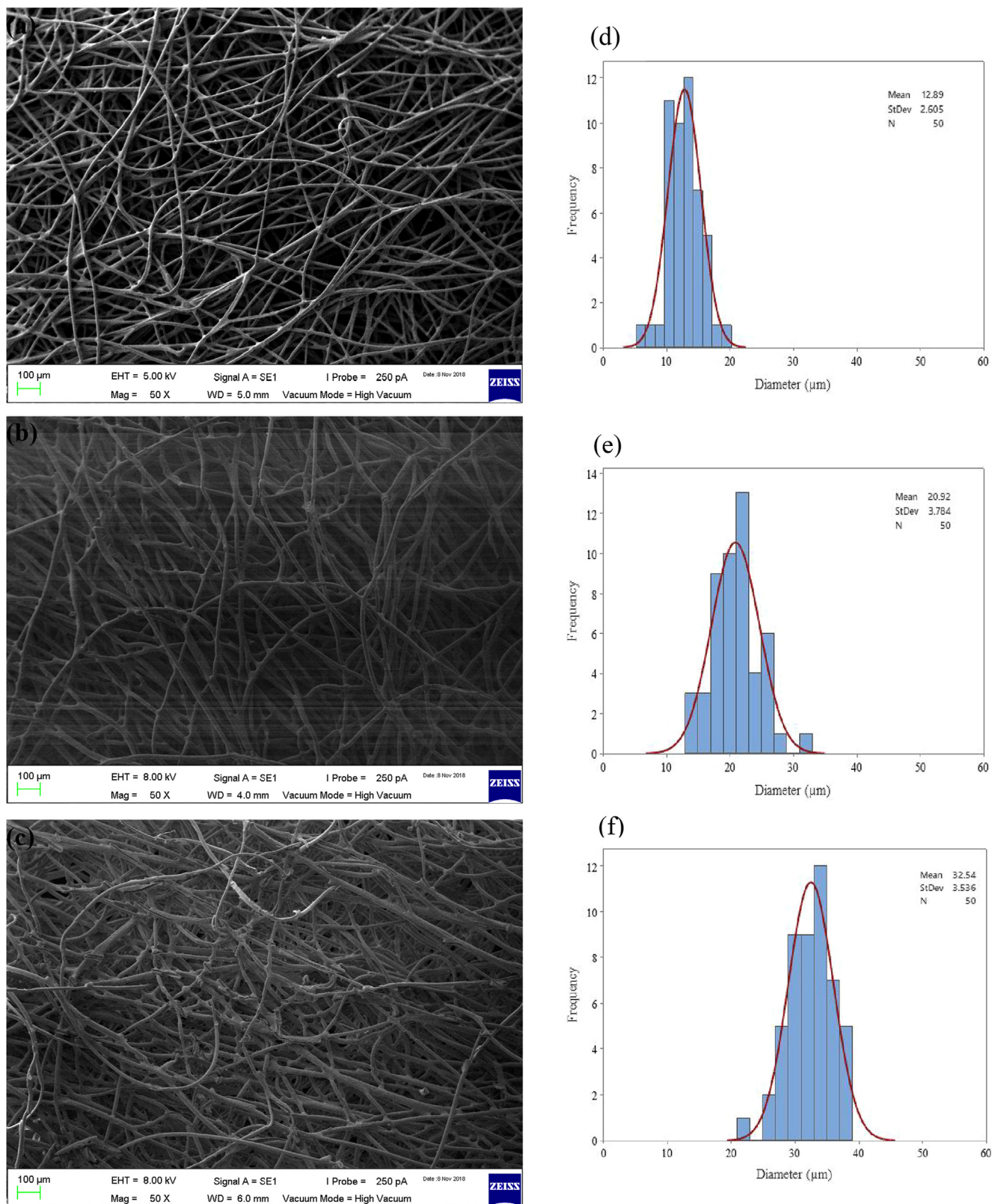
### 3.4. Changes in thermal stability

Fig. 5 shows the TGA thermograms of pristine PE/PP, PE/PP-g-PGMA and PE/PP-g-PGMA/TEPA samples. Compared to the single-step weight loss observed in the pristine PE/PP substrate starting from > 300 °C, the depolymerization of PE/PP-g-PGMA started < 300 °C following a single step decomposition pattern suggesting the presence of high compatibility between PGMA and PE/PP substrate. In the aminated sample, three-step decomposition pattern was observed with the first degradation stage started at > 100 °C and continued to 150 °C is due to the dehydration of water molecules and the desorption of pre-adsorbed CO<sub>2</sub> (Liu et al., 2013). The continuous weight loss up to ~200 °C is mostly due to the decomposition of amines. The third weight loss, which was in the range of 250–350 °C is due to the decomposition of grafted region (Xu et al., 2015). The third stage of the weight loss in PE/PP-g-PGMA/TEPA sample at 350 °C and beyond is attributed to the decomposition of the main chains of PE/PP polymer backbone.

### 3.5. Effect of reactions conditions on percent of amination

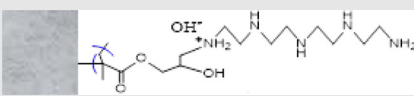
The percent of amination was calculated using equation (1) and the obtained values are presented in Table 3. Three variables including type of solvent, ratio of TEPA to solvent and the reaction time were considered. A total number of 16 experiments were suggested from Taguchi experimental design, each of the reaction took place at the boiling point of each solvent. As can be seen, water show the lowest percent of amination (0.08%) at 1:3 TEPA/water ratio and 1 h reaction time whereas isopropanol yielded the highest percent of amination (57.15) at 1:1 TEPA/isopropanol ratio and 3 h reaction time. Low amination in presence of TEPA dilution by water was also reported elsewhere (Choi, 1999). Furthermore, the ethanol also showed no significant increase in the percent of amination where amination percentage as high as 14.05% was obtained at 3:1 TEPA/ethanol ratio and 2 h reaction time. Unlike ethanol, methanol increased the percent of amination leading to an amination percentage of 43.66% at 2:1 TEPA/methanol ratio and 4 h reaction time. It can be concluded that the sequence of solvent efficiency in amination is water < ethanol < methanol < isopropanol. Hence, isopropanol was chosen as the best solvent for the amination reaction.

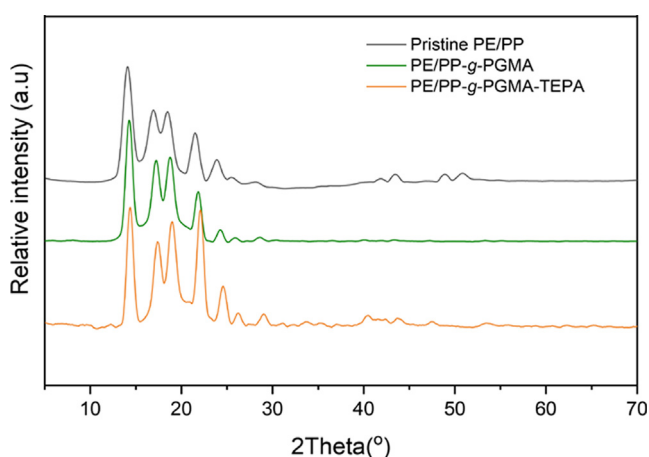
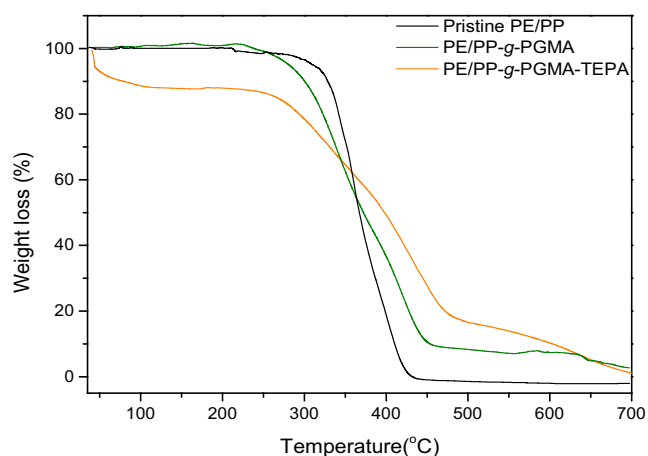
Considering solvent ratio, higher amine content led to an increase in the percent of amination with ethanol as a solvent. This is likely due to the increase in the access of TEPA to epoxy groups in the PE/PP-g-PGMA substrate. However, a slightly different trend was observed when methanol and isopropanol were used as solvents. For instance, the increase in TEPA content in methanol led to an increase in the percent of amination until it achieved 43.66% yield at a ratio of 2:1 TEPA/methanol beyond which it decreased to 32.95% with a higher content of TEPA (3:1 ratio) in the mixture. However, isopropanol showed inconsistent results as the highest percent of amination was 57.15% when the TEPA/isopropanol ratio was 1:1, but slightly decreased when the ratio was 2:1 with 49.03% of amination and again increased when the ratio was 3:1 with the percent of amination increased to 55.84%, which is almost similar to the level obtained with the ratio of 1:1.



**Fig. 3** SEM images of pristine PE/PP (a), PE/PP-g-PGMA (b) and PE/PP-g-PGMA/TEPA samples (c) together with their related histograms of diameter size distribution (d,e and f).

**Table 2** Chemical and textural properties of fibrous aminated adsorbent.

Properties	Description/value
Substrate	PE/PP
Physical form	Non-woven sheet
Ionic moiety	TEPA
Chemical structure	
Average fiber diameter ( $\mu\text{m}$ )	32.54
Amine density (mmol/g)	3.23
Surface area ( $\text{m}^2/\text{g}$ )	$2.3 \times 10^{-3}$
Pore volume ( $\text{cm}^3/\text{g}$ )	2.55
Pore radius (nm)	

**Fig. 4** XRD diffractograms of pristine PE/PP, PE/PP-g-PGMA and PE/PP-g-PGMA/TEPA samples.**Fig. 5** TGA thermograms of pristine PE/PP, PE/PP-g-PGMA and PE/PP-g-PGMA/TEPA samples.

Such inconsistency in the results could be due to the mutual changes in TEPA/isopropanol ratio and reaction time parameters at the same time. However, the longer reaction time should have led to higher percent of amination since it allows higher chances for reaction of TEPA with epoxy rings.

### 3.6. Optimization of percent of amination using Taguchi method

The main effects plots for signal-to-noise (S/N) ratio and means are shown in Fig. 6. The significance of every parameter was measured from the slope of the main effect plot. The line of high slope angle representing such parameter is more significant, which means, there is no main effect present when the line is horizontal (parallel to the x-axis). The greater the difference in the vertical position of the plot points, the greater is the magnitude of the main effect (Antony et al., 2006; Thakker et al., 2018). From the results in Fig. 6 a, it can be inferred that solvent type is more significant than the other factors. As can be seen, the highest percent of amination was obtained when isopropanol was used as a solvent whereas water showed the worst performance for amination. The reaction time showed a small effect on the S/N ratio compared to the amine to solvent ratio. The experimental runs at 2 and 3 h also had a small effect on the S/N ratio. However, longer reaction time showed higher impact on the percent of amination. It is also obvious that increasing the amount of TEPA in the reaction solution as in the case of 3:1 amine to solvent ratio led to a higher effect on the amination reaction. It can be also observed that the highest value of S/N ratio calculated at each level for each factor was selected to have the best parameters combinations to achieve the maximum percent of amination. So, to achieve the optimum percent of amination (amination efficiency), the applied parameters should be isopropanol as a solvent, 3:1 amine to solvent ratio and 4 h of reaction time.

ANOVA was conducted to identify significant parameters affecting the percent of amination and the results are presented in Table 4. A parameter with higher F-value and lower P-value has the most significant effect on the response (Liao et al., 2008; Nik et al., 2012). The solvent type appears to be more significant factor than TEPA to solvent ratio as indicated by the higher F-value of the former (25.22) compared to 18.27 for the latter. Furthermore, the P-value for the solvent is smaller (0.000) than that of the ratio value (0.001). Thus, the solvent type is the most important factor and this model can be regarded as significant since F-value for both solvent and amine/solvent ratio is  $> 1$  and P-value is  $< 0.01$ .

Fig. 7 shows the residual plots, which depicts a comparison between the experimental and predicted data. From the normal probability plot in Fig. 7 a, it seems that the plot is scattered along a straight line, which means that the experimental and predicted data have a linear relationship. Furthermore, the data are normally distributed, and the variables are affecting the response. Accordingly, the residual vs. fitted plot in Fig. 7 b shows a structure loss of the plot pattern around the residual points, which is representing the validity of the assumptions and a constant variance. Moreover, the histogram from Fig. 7 c shows that the data are not skewed and no outliers presented and the residuals vs. order from Fig. 7 d shows the time or data collection order indicating that there are systematic effects (Panda and Singh, 2013).

**Table 3** Experimental data with variation of percent of amination and reaction parameters based on Taguchi experimental design.

Experiment no.	Solvent	TEPA: solvent ratio	Reaction time (h)	Amination (%)
1	Water	1:3	1	0.08
2	Water	1:1	2	1.06
3	Water	2:1	3	1.18
4	Water	3:1	4	3.53
5	Methanol	1:3	2	19.05
6	Methanol	1:1	1	37.24
7	Methanol	2:1	4	43.66
8	Methanol	3:1	3	32.95
9	Ethanol	1:3	3	1.11
10	Ethanol	1:1	4	4.31
11	Ethanol	2:1	1	6.22
12	Ethanol	3:1	2	14.05
13	Isopropanol	1:3	4	26.35
14	Isopropanol	1:1	3	57.15
15	Isopropanol	2:1	2	49.03
16	Isopropanol	3:1	1	55.84

The Taguchi method predicts the optimum parameters required to validate the model and it suggests that higher percent of amination is desired. This experiment was performed using isopropanol as a solvent, 3:1 amine to solvent ratio and reaction time is 4 h. Thus, from the reaction, the obtained percent of amination is 70.42%, which is not only as high as predicted but also is the highest among all the results obtained from the 16 runs of experiments presented and discussed earlier. Considering the experimental run number 16, one can observe that the only different parameter was the prolonged reaction that was increased from 1 to 4 h leading to 26% increase in the percent of amination. This allowed more interactions between the aminating agent and the epoxy groups available in the PE/PP-g-PGMA adsorbent precursor leading to higher amine immobilisation (Zhuang et al., 2013). The PE/PP-g-PGMA/TEPA-V adsorbent sample obtained under optimised conditions is likely to have more CO<sub>2</sub> adsorption capacity compared counterparts with lower TEPA content. It can be concluded that the model developed from Taguchi method is proven to be capable of prediction of the percent of amination and optimisation of the reaction parameters to achieve a maximum amination efficiency in PE/PP-g-PGMA fibrous substrates.

### 3.7. CO<sub>2</sub> adsorption performance

The CO<sub>2</sub> adsorption capacity of PE/PP-g-PGMA/TEPA with the highest and lowest amine content was investigated not only to observe the impact of amine content on the CO<sub>2</sub> adsorption ability but also to validate the design of experiment created by Taguchi method at different operating pressures in various ranges up to 30 bar. The adsorbent performance was tested with pure gases (CO<sub>2</sub> and N<sub>2</sub>) followed by adsorption measurements with a binary gaseous mixture of CO<sub>2</sub>/N<sub>2</sub> containing 40% CO<sub>2</sub>. Fig. 8A shows the pure CO<sub>2</sub> adsorption isotherms for pristine PE/PP, PE/PP-g-PGMA, PE/PP-g-PGMA/TEPA3 and PE/PP-g-PGMA/TEPA14 (prepared in run 3 and 14 of Table 3), and PE/PP-g-PGMA/TEPA-V, which are the samples to validate the model from Taguchi method. Both pristine PE/PP and PE/PP-g-PGMA samples were used as adsorbent references even though they do not have functional groups, and this is to evaluate the presence

of any significant physisorption associated with strong hydrophobic nature of these samples.

As can be seen, the pristine PE/PP sample showed very low CO<sub>2</sub> adsorption yet pressure dependent isotherm with maximum adsorption capacity of 10 mg/g compared to 38 mg/g for PE/PP-g-PGMA sample at 30 bar indicating the presence of a level of affinity towards CO<sub>2</sub>. Since, such adsorbent samples do not have any functionality, thus, the observed CO<sub>2</sub> adsorption is likely to be due to physical sorption in forms of the hydrophobic associations (Van der Waals force) in fibrous substrates that was increased by the incorporation of strongly hydrophobic PGMA imparting more hydrophobicity to PE/PP fibrous sheet (Younas et al., 2016). It can be also noticed that the CO<sub>2</sub> adsorption capacity of PE/PP-g-PGMA/TEPA3 with an amination efficiency of 1.18% (after H<sub>2</sub>O/TEPA mixture treatment) was as low as 41 mg/g at 30 bar, which is slightly higher than that of PE/PP-g-PGMA. This suggests that the hydrophobic fibrous structure have a more important role than the TEPA functionalities in this sample. In other words, physisorption is predominantly controlling the adsorption behavior of this slightly aminated sample having a curve shape matching those of pristine and grafted samples and resembling multi-layer adsorption.

At higher amination levels of 57.15% and 70.42%, the shape of the pressure-dependent curves (isotherms) started to shift towards Type-I suggesting a monolayer adsorption dominated by chemisorption. The CO<sub>2</sub> adsorption capacity of PE/PP-g-PGMA/TEPA14 (obtained from isopropanol/TEPA mixture treatment without optimization) almost doubled to 80 mg/g at 30 bar, which was considerably increased to 117 mg/g for PE/PP-g-PGMA/TEPA-V (obtained from isopropanol/TEPA mixture treatment optimization) due to the increase in basic TEPA sites causing a stronger affinity to CO<sub>2</sub> which has an acidic nature. When this adsorbent was tested for pure N<sub>2</sub> adsorption under similar conditions, it showed a negligible affinity to CO<sub>2</sub> as indicated by the tiny adsorption capacity ( $\geq 1.29$  mg/g) at various pressures up to 30 bar as shown in Fig. 8B. This indicates that the adsorbent is highly selective to CO<sub>2</sub>.

The adsorption behavior of binary CO<sub>2</sub>/N<sub>2</sub> gaseous mixture on 5 adsorbent samples at various pressures were measured and is represented by adsorption isotherms depicted in

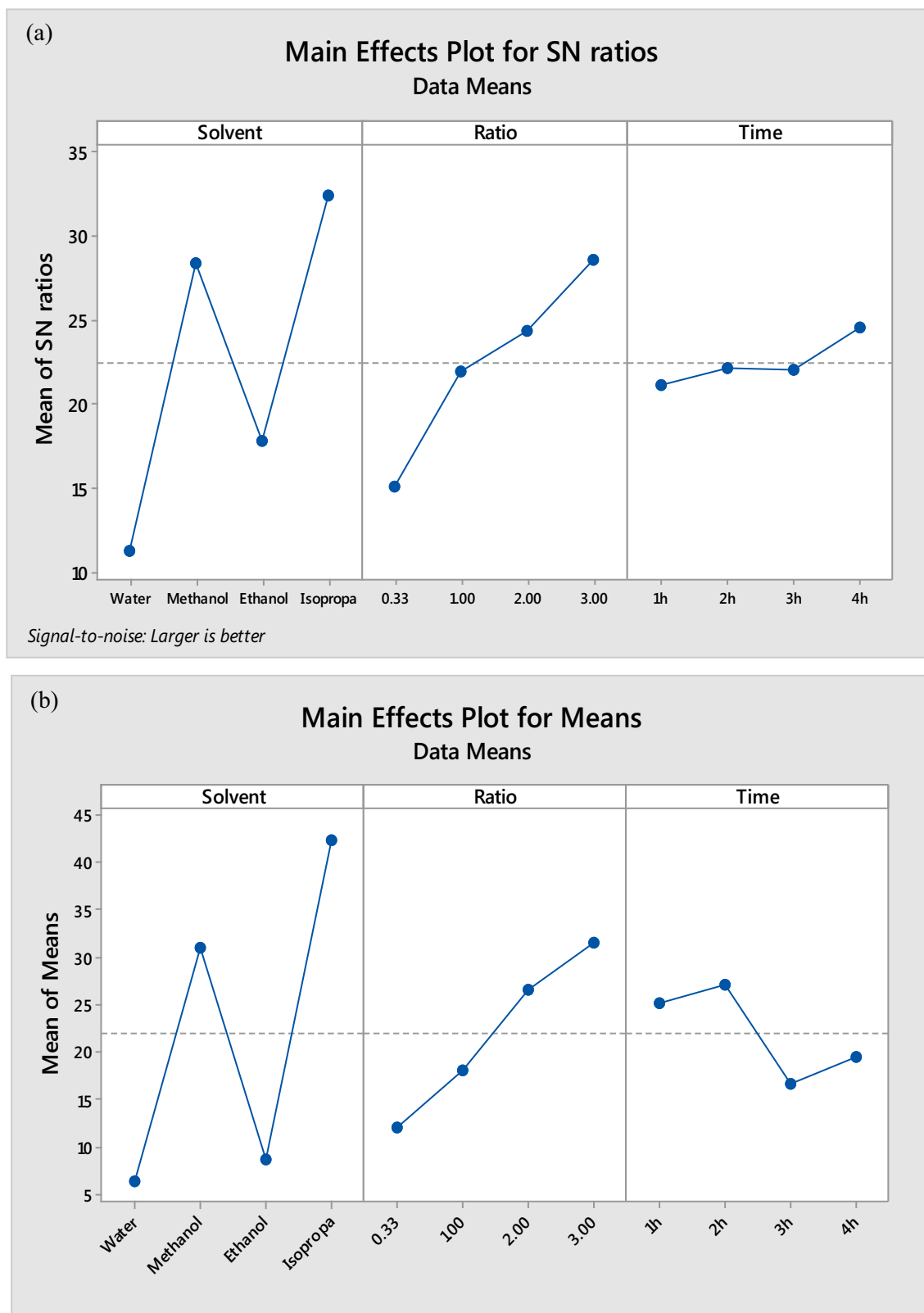
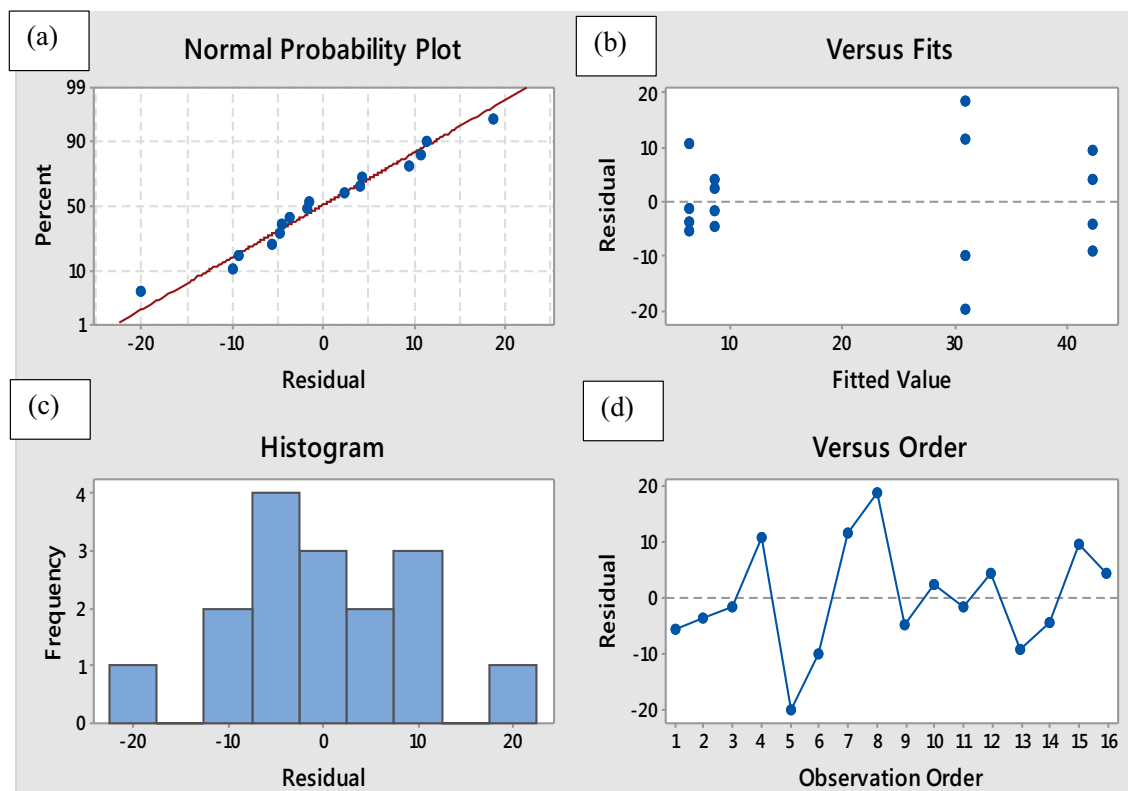


Fig. 6 Main effects plots for SN ratios (a) and main effects plots for means (b) for reaction parameters.

Fig. 9. As in pure gases, the adsorption has a pressure-dependant behavior and the performance followed pure CO<sub>2</sub> gas increasing trend. However, the performance of all samples is approximately reduced by 44% upon using a gas mixture of

40% CO<sub>2</sub> with 60% N<sub>2</sub>. The reduction in CO<sub>2</sub> sorption in gas mixture is due to the competition between CO<sub>2</sub> and N<sub>2</sub> gases which led to a reduction in the accessibility of amine groups for CO<sub>2</sub> molecules (Rodríguez et al., 2019). Moreover, PE/

Source	DF	Adj SS	Adj MS	F-value	P-value
Regression	4	4536.2	1134.04	23.48	0.000
Ratio	1	882.4	882.39	18.27	0.001
Solvent	3	3653.8	1217.92	25.22	0.000
Error	11	531.2	48.29		
Total	15	5067.3			



**Fig. 7** Plots of normal probability, variation of the standardized residuals with fitted values, histogram of variation frequency with residuals and variation of the standardized residuals with observed order values of the data.

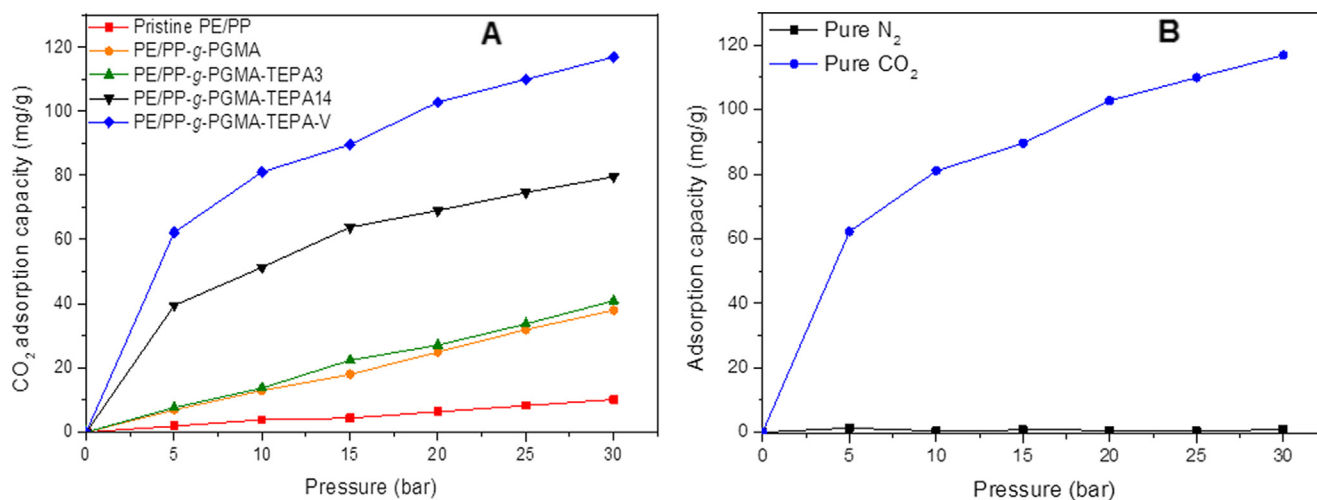
PP-g-PGMA/TEPA-V showed the highest performance at all pressures.

Table 5 shows the variation of the adsorption selectivity of best adsorbent, which was estimated at various pressures at 30 °C. The PE/PP-g-PGMA/TEPA-V adsorbent exhibited high adsorption selectivity of CO<sub>2</sub> over N<sub>2</sub> at all pressures with the highest value of 1194 obtained at 5 bar which decreased to 136 at 30 bar. These observations indicate that a large amount of CO<sub>2</sub> can be adsorbed at low pressures compared to N<sub>2</sub>, which is scarcely adsorbed. This indicated that the interaction between polar surface of the adsorbent and quadrupolar molecule of CO<sub>2</sub> is favourably occurred at low pressure which is explained by the high selectivity at 5 bar operating pressure. Similar observation was reported for selective adsorption of CO<sub>2</sub> from a mixture with CH<sub>4</sub> (Tammanloo et al., 2014). The high selectivity of this adsorbent is caused by the strong affinity of CO<sub>2</sub> towards TEPA groups unlike N<sub>2</sub>. Moreover, the

variation in the selectivity depends on level of accessibility to TEPA groups. It is noteworthy mentioning that the adsorption selectivity of such fibrous aminated adsorbent is not only reported for first time but also the obtained selectivity values are interestingly high and can match those of established CO<sub>2</sub> adsorbents (Varghese and Karanikolos, 2020; Yang et al., 2017). It can be concluded PE/PP-g-PGMA/TEPA-V is a potential adsorbent for separation of CO<sub>2</sub> from its mixtures with N<sub>2</sub>.

### 3.8. TEPA utilisation efficiency and selectivity of adsorbents

The experimental adsorption capacity is compared with the theoretical adsorption capacity for 3 adsorbents with different TEPA content and the data is present in Fig. 10A. The experimental adsorption capacities of the two adsorbents with high TEPA content were smaller than their corresponding theoret-



**Fig. 8** Variation of adsorption with pressure for: A) pure CO<sub>2</sub> on pristine, grafted substrates and various adsorbents and for B) pure CO<sub>2</sub> and N<sub>2</sub> adsorption on PE/PP-g-PGMA/TEPA-V at 30 °C.

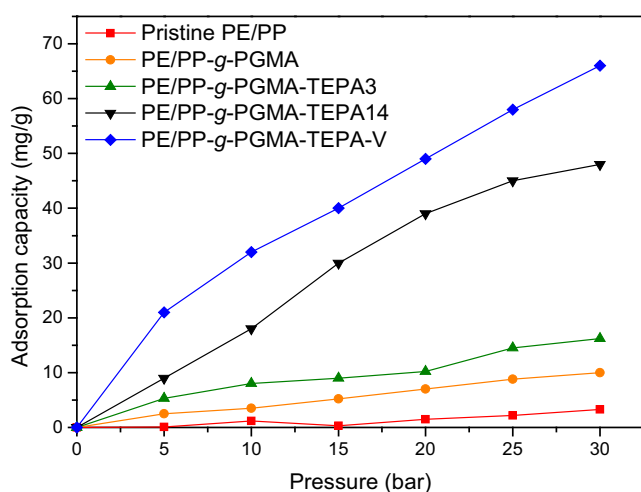


**Fig. 9** Variation of CO<sub>2</sub> adsorption with pressure on pristine and grafted substrates and adsorbents for a mixture of CO<sub>2</sub> and N<sub>2</sub> containing 40% CO<sub>2</sub>.

**Table 5** Variation of adsorption selectivity for CO<sub>2</sub>/N<sub>2</sub> with pressure at 30 °C for PE/PP-g-PGMA/TEPA-V.

Pressure (bar)	Adsorption selectivity
5	1194
10	281
15	160
20	181
25	189
30	136

ical adsorption capacities but maintained equal differences. For instance, PE/PP-g-PGMA/TEPA-V (70.42 amine %) and PE/PP-g-PGMA/TEPA14 (57.15 amine %) showed about

47% lower adsorption capacities than their corresponding theoretical values that were 221 and 149 mg/g, respectively. Such difference seems to be reasonable taking the low surface area of the present fibrous adsorbent into consideration. The unusual behavior of PE/PP-g-PGMA/TEPA3 in which the theoretical adsorption capacity was found to be inferior to that of experimental value by 85.3% is caused by the extremely low amination efficiency of 1.18% leaving the physical adsorption observed in the hydrophobic grafted sample to play a bigger role in CO<sub>2</sub> adsorption than the tiny TEPA content. The increase in the amination level to 57.15% and above imparted strong hydrophilic moieties to the adsorbent surface leading to the dominance of chemical adsorption and the suppression of the physical adsorption.

The TEPA utilization efficiency or CO<sub>2</sub> adsorption capacity per unit TEPA ( $Q$ ) of 3 functionalised adsorbents with different amination percentages is presented in Fig. 10B. As can be seen,  $Q$  increased from 210 to 310 mg/g with the rise in the TEPA content from 1.18% in PE/PP-g-PGMA/TEPA3 to 57.15% in PE/PP-g-PGMA/TEPA14. The physisorption of CO<sub>2</sub> was excluded from the former sample. The increase in TEPA content to 70.42% in PE/PP-g-PGMA/TEPA-V sample showed almost no change in  $Q$  and stands at 308 mg/g. This trend is most likely attributed to the presence of incomplete amination level (i.e., not achieving 100%) in the two samples despite the variation of amination percentage. This allowed more access to amine sites with the pressure increase by enhancing the CO<sub>2</sub> diffusion that overcome the mass transfer limitation. This observation suggests that TEPA utilization efficiency is mainly dependent on the content and the access to amine sites which plays a crucial role in determining the overall adsorption capacity of the present adsorbent. Similar observations were reported for nanofibrous polypropylene-based adsorbents containing PGMA grafts modified with various amines (Abbasi et al., 2019a; Lin et al., 2013).

### 3.9. Regeneration of PE/PP-g-PGMA/TEPA-V adsorbent

The stability of PE/PP-g-PGMA/TEPA-V sample was evaluated for 11 adsorption/desorption cycles and the results are

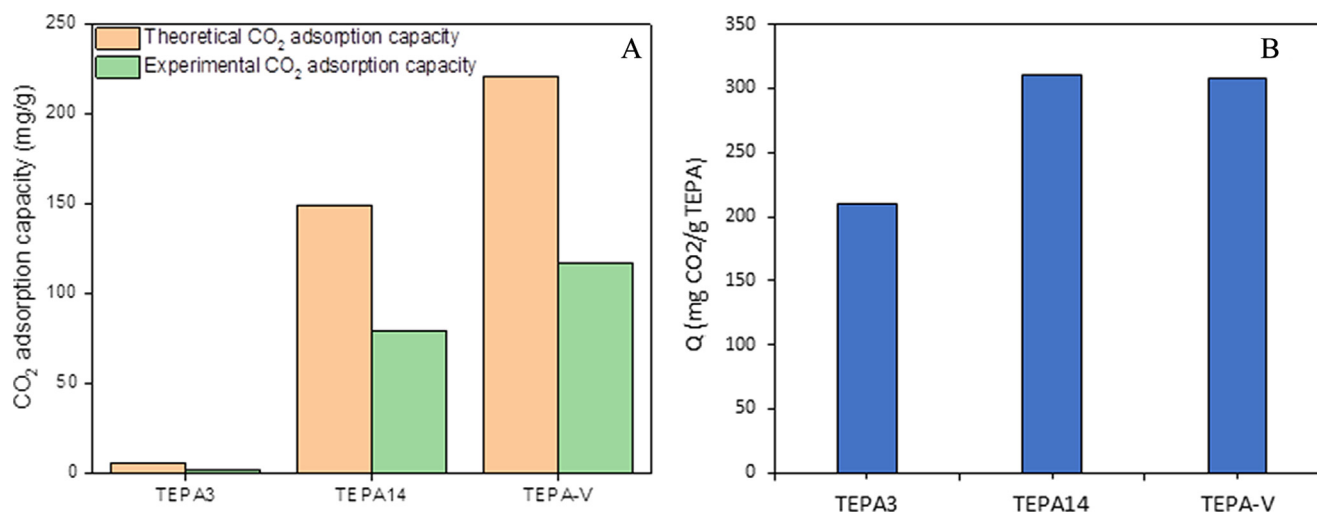


**Fig. 10** Experimental and theoretical CO<sub>2</sub> adsorption capacities (A) and TEPA utilisation efficiency (B) on 3 adsorbents with different amination levels.

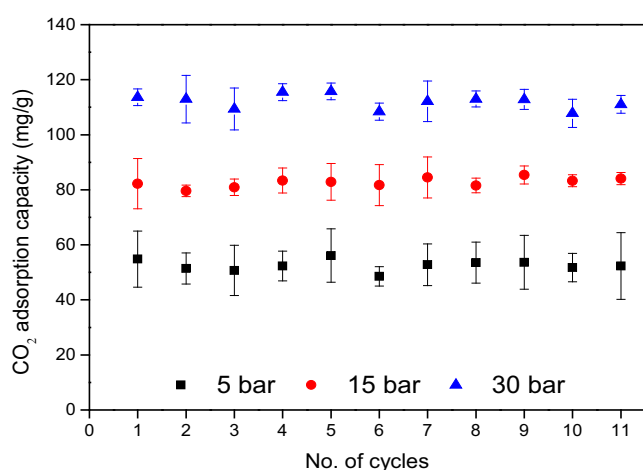


**Fig. 11** CO<sub>2</sub> adsorption/desorption cycles for PE/PP-g-PGMA/TEPA-V at different pressures.

present in Fig. 11. The adsorption was conducted at a temperature of 30 °C with a pure CO<sub>2</sub> and a flowrate of 500 ml/min and the adsorbent was regenerated by placing it inside the sample container of MSB and heating to 80 °C for 4.5 h under vacuum conditions until a constant weight was obtained in the adsorbent. The adsorbent showed a reasonable stability with an average adsorption capacity of 114 mg/g (~3% loss) after 11 cycles at a pressure of 30 bar. Such negligible loss in the adsorption capacity is possibly due to the leaching of few unbound chains that were likely occluded among PGMA/TEPA grafts covalently bonded to the surface of the adsorbent. Furthermore, the applied desorption method involving a combination of vacuum and heating treatments was effective in reversing the chemical interaction between CO<sub>2</sub> and PE/PP-g-PGMA/TEPA-V and the adsorbent can be used for prolonged cyclic operation. It can be concluded that the performance of PE/PP-g-PGMA/TEPA-V adsorbent is almost retained after 11 adsorption/desorption cycles suggesting that

it is stable enough with an excellent regeneration for column and scaled application of CO<sub>2</sub> capture.

Table 6 shows a comparison between the adsorbent developed in this study and various researched polymeric adsorbents. As can be seen, the present adsorbent has very good adsorption capacity compared to all aminated adsorbents of same category. Considering the nature of present adsorbent and the method used of its preparation, its properties including stability, regeneration, and its chemisorption adsorption mechanism, it can be suggested that PE/PP-g-PGMA/TEPA-V is a promising adsorbent for CO<sub>2</sub> capture. Moreover, the adopted RIGC preparation method is not only environmentally friendly but also cost effective and versatile in allowing the use of various waste fibers and fabrics as substrates for developing CO<sub>2</sub> adsorbents. Finally, the fibrous nature of the present adsorbent provides advantages in its handling in industrial application including reduction of pressure loss, where competing adsorbents in particulate forms such as COP, zeolite, COF and glucose-based carbon having higher CO<sub>2</sub> adsorption performance are likely to undergo serious challenges such as dustiness, clogging, channelling and pressure drop when applied in columns (Pu et al., 2018).

#### 4. Conclusion

An interesting fibrous adsorbent made of PGMA/TEPA grafted PE/PP fibrous sheet and containing a maximum amount of TEPA was successfully prepared and tested for CO<sub>2</sub> adsorption. The amination efficiency of PE/PP-g-PGMA precursor substrates was optimized by controlling the reaction parameters such as type of solvent, amine to solvent ratio and reaction time using Taguchi method. The parameters' optimization increased the amination efficiency from 57.15% (obtained with 1:1 isopropanol/TEPA ratio at 3 h) to 70.42% (obtained with 3:1 isopropanol/TEPA ratio at 4 h) leading to a remarkable increase in the CO<sub>2</sub> adsorption capacity from 80 to 117 mg/g in the adsorbent. Thus, Taguchi method is proven to be highly effective in optimization of reaction parameters and endowing the maximum amination

**Table 6** Comparison between performance of present adsorbent and solid amine adsorbents reported in literature.

Materials	Functional group	Adsorption method	CO <sub>2</sub> adsorption capacity (mg/g)	Temperature (°C)	CO <sub>2</sub> composition (%)	Refs.
PMMA	PEI	Column	155	45	100	(Gray et al., 2009)
Viscose-PGMA	TETA	Column	103	25	20	(Lin et al., 2013)
PP-g-PGMA (microfibers)	TEPA	Column	99	30	15	(Zhuang et al., 2013)
Porous polystyrene resin	TEPA	Column	53	30	10	(Liu et al., 2017)
PP-g-PGMA (nanofibers)	EA	Column	126	30	15	(Abbasi et al., 2019b)
PP-g-PGMA (nanofibers)	DEA	Column	91	30	15	(Abbasi et al., 2019a)
PP-g-PGMA (nanofibers)	TEA	Column	41	30	15	(Abbasi et al., 2019b)
Ion exchange resin	Benzyl amine	Column	79	30	10	(Alesi and Kitchin, 2012)
Polyamide-6/CNT nanofibers	PEI	Column	71	25	100	(Zainab et al., 2017)
PE/PP-g-PVAm	–	MSB	60	30	100	(Zubair et al., 2020)
PE/PP-g-PGMA	TEPA	MSB	117	30	100	This study

efficiency. The PE/PP-g-PGMA/TEPA-V adsorbent was found to be highly selective for CO<sub>2</sub> over N<sub>2</sub> and has a high amine utilization efficiency coupled with a competitive adsorption capacity. Furthermore, the adsorbent was found to have very good stability and can be easily regenerated at 80 °C rendering it suitable for column and scaled CO<sub>2</sub> capture applications.

### Declaration of Competing Interest

The authors declare that they have no known competing financial interests or personal relationships that could have appeared to influence the work reported in this paper.

### Acknowledgement

This work was supported by Malaysia Thailand Joint Authority (MTJA) under vote no. 4C116. MMN is debt for the partial support for this work from International Atomic Energy Agency (IAEA) under from coordinated research projects (CRP # F22072).

### References

- Abbasi, A., Nasef, M.M., Babadi, F.E., Faridi-Majidi, R., Takeshi, M., Abouzari-Lotf, E., Choong, T., Somwangthanaroj, A., Kheawhom, S., 2019a. Carbon dioxide adsorption on grafted nanofibrous adsorbents functionalized using different amines. *Front. Energy Res.* 7, 1–14. <https://doi.org/10.3389/fenrg.2019.00145>.
- Abbasi, A., Nasef, M.M., Faridi-Majidi, R., Etesami, M., Takeshi, M., Abouzari-Lotf, E., 2018. Highly flexible method for fabrication of poly (Glycidyl Methacrylate) grafted polyolefin nanofiber. *Radiat. Phys. Chem.* 151, 283–291. <https://doi.org/10.1016/j.radphyschem.2018.07.002>.
- Abbasi, A., Nasef, M.M., Kheawhom, S., Faridi-majidi, R., Takeshi, M., Abouzari-lotf, E., Choong, T., 2019b. Amine functionalized radiation induced grafted polyolefin nanofibers for CO<sub>2</sub> adsorption. *Radiat. Phys. Chem.* 156, 58–66. <https://doi.org/10.1016/j.radphyschem.2018.10.015>.
- Abu-Zahra, M.R.M., Abbas, Z., Singh, P., Feron, P., 2013. Carbon dioxide post-combustion capture: solvent technologies overview, status and future directions. *Mater. Process. Energy Commun. Curr. Res. Technol. Dev.*, 923–934
- Alesi, W.R., Kitchin, J.R., 2012. Evaluation of a primary amine-functionalized ion-exchange resin for CO<sub>2</sub> capture. *Ind. Eng. Chem. Res.* 51, 6907–6915. <https://doi.org/10.1021/ie300452c>.
- Andreoli, E., 2017. Materials and processes for carbon dioxide capture and utilisation. *J. Carbon Res.* 3, 16. <https://doi.org/10.3390/c3020016>.
- Antony, J., Perry, D., Wang, C., Kumar, M., 2006. An application of Taguchi method of experimental design for new product design and development process. *Assem. Autom.* 26, 18–24. <https://doi.org/10.1108/01445150610645611>.
- Choi, S., 1999. Adsorption of Pb<sup>2+</sup>, Cu<sup>2+</sup> and Co<sup>2+</sup> by polypropylene fabric and polyethylene hollow fiber modified by radiation-induced 16, 241–247.
- Dao, D.S., Yamada, H., Yogo, K., 2020. Enhancement of CO<sub>2</sub> adsorption/desorption properties of solid sorbents using tetraethylenepentamine/diethanolamine blends. *ACS Omega* 5, 23533–23541. <https://doi.org/10.1021/acsomega.0c01515>.
- Davis, R., John, P., 2018. Application of Taguchi-based design of experiments for industrial chemical processes. *Stat. Approaches With Emphas. Des. Exp. Appl. to Chem. Process.* <https://doi.org/10.5772/intechopen.69501>.

- Fujii, T., Nakagawa, S., Sato, Y., Inomata, H., Hashida, T., 2010. Sorption characteristics of CO<sub>2</sub> on rocks and minerals in storing CO<sub>2</sub> processes. *Nat. Resour.* 01, 1–10. <https://doi.org/10.4236/nr.2010.11001>.
- Gray, M.L., Hoffman, J.S., Hreha, D.C., Fauth, D.J., Hedges, S.W., Champagne, K.J., Pennline, H.W., 2009. Parametric study of solid amine sorbents for the capture of carbon dioxide. *Energy Fuels* 23, 4840–4844. <https://doi.org/10.1021/ef9001204>.
- Graziano, A., Jaffer, S., Sain, M., 2018. Review on modification strategies of polyethylene/polypropylene immiscible thermoplastic polymer blends for enhancing their mechanical behavior. *J. Elastomers Plast.* <https://doi.org/10.1177/0095244318783806>.
- Guo, Y., Luo, L., Zheng, Y., Zhu, T., 2020. Optimization of CO<sub>2</sub> adsorption on solid-supported amines and thermal regeneration mode comparison. *ACS Omega* 5, 9641–9648. <https://doi.org/10.1021/acsomega.9b03374>.
- Hashim, K., 1998. Cation exchange membranes by radiation-induced graft copolymerization of styrene onto PFA copolymer films. I. Preparation and characterization of the graft copolymer. *J. Appl. Polym. Sci.* 73, 2095–2102.
- Irani, M., Fan, M., Ismail, H., Tuwati, A., Dutcher, B., Russell, A.G., 2015. Modified nanosepiolite as an inexpensive support of tetraethylenepentamine for CO<sub>2</sub> sorption. *Nano Energy* 11, 235–246. <https://doi.org/10.1016/j.nanoen.2014.11.005>.
- Jafari, B., Rahimi, M.R., Ghaedi, M., Dashtian, K., Mosleh, S., 2018. CO<sub>2</sub> capture by amine-based aqueous solution containing atorvastatin functionalized mesocellular silica foam in a counter-current rotating packed bed: Central composite design modeling. *Chem. Eng. Res. Des.* 129, 64–74. <https://doi.org/10.1016/j.cherd.2017.11.005>.
- Jahandar Lashaki, M., Khiavi, S., Sayari, A., 2019. Stability of amine-functionalized CO<sub>2</sub> adsorbents: A multifaceted puzzle. *Chem. Soc. Rev.* 48, 3320–3405. <https://doi.org/10.1039/c8cs00877a>.
- Kavakli, C., Akkaş Kavakli, P., Güven, O., 2014. Preparation and characterization of glycidyl methacrylate grafted 4-amino-1,2,4-triazole modified nonwoven fiber adsorbent for environmental application. *Radiat. Phys. Chem.* 94, 111–114. <https://doi.org/10.1016/j.radphyschem.2013.07.018>.
- Kavakli, C., Barsbay, M., Tilki, S., Güven, O., Kavakli, P.A., 2016. Activation of polyethylene/polypropylene nonwoven fabric by radiation-induced grafting for the removal of Cr(VI) from aqueous solutions. *Water. Air. Soil Pollut.* 227. <https://doi.org/10.1007/s11270-016-3184-5>.
- Leung, D.Y.C., Caramanna, G., Maroto-Valer, M.M., 2014. An overview of current status of carbon dioxide capture and storage technologies. *Renew. Sustain. Energy Rev.* 39, 426–443. <https://doi.org/10.1016/j.rser.2014.07.093>.
- Liao, H.-T., Shie, J.-R., Yang, Y.-K., 2008. Applications of Taguchi and design of experiments methods in optimization of chemical mechanical polishing process parameters. *Int. J. Adv. Manuf. Technol.* 38, 674–682. <https://doi.org/10.1007/s00170-007-1124-7>.
- Lin, R., Zhuang, L., Xu, X., Chen, S., 2013. Design of a viscose based solid amine fiber: Effect of its chemical structure on adsorption properties for carbon dioxide. *J. Colloid Interface Sci.* 407, 425–431. <https://doi.org/10.1016/j.jcis.2013.06.029>.
- Liu, F., Chen, S., Gao, Y., Xie, Y., 2017. Synthesis and CO<sub>2</sub> adsorption behavior of amine-functionalized porous polystyrene adsorbent. *J. Appl. Polym. Sci.* 134, 1–7. <https://doi.org/10.1002/app.45046>.
- Liu, L., Chen, H., Shiko, E., Fan, X., Zhou, Y., Zhang, G., Luo, X., Hu, X. (Eric), 2018. Low-cost DETA impregnation of acid-activated sepiolite for CO<sub>2</sub> capture. *Chem. Eng. J.* 353, 940–948. <https://doi.org/10.1016/j.cej.2018.07.086>.
- Liu, Z., Teng, Y., Zhang, K., Cao, Y., Pan, W., 2013. CO<sub>2</sub> adsorption properties and thermal stability of different amine-impregnated MCM-41 materials. *J. Fuel Chem. Technol.* 41, 469–475. [https://doi.org/10.1016/S1872-5813\(13\)60025-0](https://doi.org/10.1016/S1872-5813(13)60025-0).
- Luis Míguez, J., Porteiro, J., Pérez-Orozco, R., Patiño, D., Rodríguez, S., 2018. Evolution of CO<sub>2</sub> capture technology between 2007 and 2017 through the study of patent activity. *Appl. Energy* 211, 1282–1296. <https://doi.org/10.1016/j.apenergy.2017.11.107>.
- Luo, S., Chen, Siyu, Chen, Y., Chen, Shuixia, Ma, N., Wu, Q., 2016. Sisal fiber-based solid amine adsorbent and its kinetic adsorption behaviors for CO<sub>2</sub>. *RSC Adv.* 6, 72022–72029. <https://doi.org/10.1039/C6RA14627A>.
- Nasef, M.M., Abbasi, A., Ting, T.M., 2014a. New CO<sub>2</sub> adsorbent containing aminated poly(glycidyl methacrylate) grafted onto irradiated PE-PP nonwoven sheet. *Radiat. Phys. Chem.* 103, 72–74. <https://doi.org/10.1016/j.radphyschem.2014.05.031>.
- Nasef, M.M., Güven, O., 2012. Radiation-grafted copolymers for separation and purification purposes: Status, challenges and future directions. *Prog. Polym. Sci.* 37, 1597–1656. <https://doi.org/10.1016/j.progpolymsci.2012.07.004>.
- Nasef, M.M., Ting, T.M., Abbasi, A., Layeghi-moghaddam, A., Sara Alinezhad, S., Hashim, K., 2014b. Radiation grafted adsorbents for newly emerging environmental applications. *Radiat. Phys. Chem.* 118, 55–60. <https://doi.org/10.1016/j.radphyschem.2015.02.025>.
- Nik, O.G., Sadrzadeh, M., Kaliaguine, S., 2012. Surface grafting of FAU/EMT zeolite with (3-aminopropyl)methyldiethoxysilane optimized using Taguchi experimental design. *Chem. Eng. Res. Des.* 90, 1313–1321. <https://doi.org/10.1016/j.cherd.2011.12.008>.
- Othman, N.A.F., Selambakkannu, S., Abdullah, T.A.T., Hoshina, H., Sattayaporn, S., Seko, N., 2019. Selectivity of copper by amine-based ion recognition polymer adsorbent with different aliphatic amines. *Polymers (Basel)*. 11. <https://doi.org/10.3390/polym11121994>.
- Panda, A.K., Singh, R.K., 2013. Optimization of Process Parameters by Taguchi Method : Catalytic degradation of polypropylene to liquid fuel 50–54.
- Petrovic, B., Gorbounov, M., Masoudi Soltani, S., 2020. Influence of surface modification on selective CO<sub>2</sub> adsorption: A technical review on mechanisms and methods. *Microporous Mesoporous Mater.* 110751. <https://doi.org/10.1016/j.micromeso.2020.110751>.
- Pu, S., Wang, J., Li, L., Zhang, Z., Bao, Z., Yang, Q., Yang, Y., Xing, H., Ren, Q., 2018. Performance comparison of metal-organic framework extrudates and commercial zeolite for ethylene/ethane separation. *Ind. Eng. Chem. Res.* 57, 1645–1654. <https://doi.org/10.1021/acs.iecr.7b04391>.
- Rodríguez, E., Arqués, J.L., Rodríguez, R., Nuñez, M., Medina, M., Talarico, T.L., Casas, I.A., Chung, T.C., Dobrogosz, W.J., Axelsson, L., Lindgren, S.E., Dobrogosz, W.J., Kerkeni, L., Ruano, P., Delgado, L.L., Picco, S., Villegas, L., Tonelli, F., Merlo, M., Rigau, J., Diaz, D., Masuelli, M., 2019. Experimental study of adsorption on activated carbon for CO<sub>2</sub> capture. *Intech* 32, 137–144.
- Schell, J., Casas, N., Pini, R., Mazzotti, M., 2012. Pure and binary adsorption of CO<sub>2</sub>, H<sub>2</sub>, and N<sub>2</sub> on activated carbon. *Adsorption* 18, 49–65. <https://doi.org/10.1007/s10450-011-9382-y>.
- Selin, Ş., Emik, S., 2018. Fast and highly efficient removal of 2, 4-D using amino-functionalized poly (glycidyl methacrylate) adsorbent: optimization, equilibrium, kinetic and thermodynamic studies. *J. Mol. Liq.* 260, 195–202. <https://doi.org/10.1016/j.molliq.2018.03.091>.
- Sharif, J., Mohamad, S.F., Fatimah Othman, N.A., Bakaruddin, N. A., Osman, H.N., Güven, O., 2013. Graft copolymerization of glycidyl methacrylate onto delignified kenaf fibers through pre-irradiation technique. *Radiat. Phys. Chem.* 91, 125–131. <https://doi.org/10.1016/j.radphyschem.2013.05.035>.
- Songolzadeh, M., Soleimani, M., Takht Ravanchi, M., Songolzadeh, R., 2014. Carbon dioxide separation from flue gases: A technological review emphasizing reduction in greenhouse gas emissions. *Sci. World J.* 2014. <https://doi.org/10.1155/2014/828131>.
- Tamnanloo, J., Fatemi, S., Golmakani, A., 2014. Binary equilibrium adsorption data and comparison of zeolites with activated carbon

- for selective adsorption of CO<sub>2</sub> from CH<sub>4</sub>. *Adsorpt. Sci. Technol.* 32, 707–716. <https://doi.org/10.1260/0263-6174.32.9.707>.
- Thakker, M.R., Parikh, J.K., Desai, M.A., 2018. Synergism between ionic liquid and ultrasound for greener extraction of geraniol: Optimization using different statistical tools, comparison and prediction. *Chem. Eng. Res. Des.* 134, 162–171. <https://doi.org/10.1016/j.cherd.2018.04.003>.
- Thouchprasitchai, N., Pintuyothin, N., Pongstabodee, S., 2017. Optimization of CO<sub>2</sub> adsorption capacity and cyclical adsorption/desorption on tetraethylenepentamine-supported surface-modified hydrotalcite. *J. Environ. Sci.* 65, 293–305. <https://doi.org/10.1016/j.jes.2017.02.015>.
- Varghese, A.M., Karanikolos, G.N., 2020. CO<sub>2</sub> capture adsorbents functionalized by amine – bearing polymers: A review. *Int. J. Greenh. Gas Control* 96,. <https://doi.org/10.1016/j.ijggc.2020.103005> 103005.
- Wang, Y., Guo, T., Hu, X., Hao, J., Guo, Q., 2020. Mechanism and kinetics of CO<sub>2</sub> adsorption for TEPA-impregnated hierarchical mesoporous carbon in the presence of water vapor. *Powder Technol.* 368, 227–236. <https://doi.org/10.1016/j.powtec.2020.04.062>.
- Xu, T., Wu, Q., Chen, S., Deng, M., 2015. Preparation of polypropylene based hyperbranched absorbent fibers and the study of their adsorption of CO<sub>2</sub>. *RSC Adv.* 5, 32902–32908. <https://doi.org/10.1039/C5RA02182K>.
- Yang, H., Luo, M., Chen, X., Zhao, X., Lin, J., Hu, D., Li, D., Bu, X., Feng, P., Wu, T., 2017. Cation-exchanged zeolitic chalcogenides for CO<sub>2</sub> adsorption. *Inorg. Chem.* 56, 14999–15005. <https://doi.org/10.1021/acs.inorgchem.7b02307>.
- Younas, M., Sohail, M., Kong, L.L., Bashir, M.J.K., Sethupathi, S., 2016. Feasibility of CO<sub>2</sub> adsorption by solid adsorbents: a review on low-temperature systems. *Int. J. Environ. Sci. Technol.* 13, 1839–1860. <https://doi.org/10.1007/s13762-016-1008-1>.
- Zainab, G., Iqbal, N., Babar, A.A., Huang, C., Wang, X., Yu, J., Ding, B., 2017. Free-standing, spider-web-like polyamide/carbon nanotube composite nanofibrous membrane impregnated with polyethyleneimine for CO<sub>2</sub> capture. *Compos. Commun.* 6, 41–47. <https://doi.org/10.1016/j.coco.2017.09.001>.
- Zhang, G., Zhao, P., Hao, L., Xu, Y., Cheng, H., 2019. Separation and Purification Technology A novel amine double functionalized adsorbent for carbon dioxide capture using original mesoporous silica molecular sieves as support. *Sep. Purif. Technol.* 209, 516–527. <https://doi.org/10.1016/j.seppur.2018.07.074>.
- Zhuang, L., Chen, S., Lin, R., Xu, X., 2013. Preparation of a solid amine adsorbent based on polypropylene fiber and its performance for CO<sub>2</sub> capture. *J. Mater. Res.* 28, 2881–2889. <https://doi.org/10.1557/jmr.2013.278>.
- Zubair, N.A., Nasef, M.M., Mohamad, N.A., Abouzari-Lotf, E., Ting, T.M., Abdullah, E.C., 2020. Kinetic studies of radiation induced grafting of N-vinylformamide onto polyethylene/polypropylene fibrous sheets and testing its hydrolysed copolymer for CO<sub>2</sub> adsorption. *Radiat. Phys. Chem.* 171. <https://doi.org/10.1016/j.radphyschem.2020.108727>.